Journal of Geophysical Research: Earth Surface

RESEARCH ARTICLE
10.1029/2018JF004654

Analytical Solution for Anomalous Diffusion of Bedload Tracers Gradually Undergoing Burial

Zi Wu[1,2,3], Efi Foufoula-Georgiou[1,3], Gary Parker[4], Arvind Singh[5], Xudong Fu[2], and Guangqian Wang[2]

[1]Department of Civil and Environmental Engineering, University of California Irvine, Irvine, CA, USA, [2]State Key Laboratory of Hydroscience and Engineering; Department of Hydraulic Engineering, Tsinghua University, Beijing, China, [3]National Center for Earth-Surface Dynamics and St. Anthony Falls Laboratory, University of Minnesota, Minneapolis, MN, USA, [4]Department of Civil and Environmental Engineering and Department of Geology, Hydrosystems Laboratory, University of Illinois at Urbana-Champaign, Urbana, IL, USA, [5]Department of Civil, Environmental and Construction Engineering, University of Central Florida, Orlando, FL, USA

Key Points:
- A modified active layer formulation allows analytical treatment of tracer burial during transport
- Analytical solutions reproduce the advective slowdown and superdiffusion obtained by numerical simulations
- Intermediate timescale superdiffusion is related to an advection-induced scaling ($\propto t^3$) caused by tracer burial

Correspondence to:
Z. Wu,
wuzi@pku.edu.cn

Citation:
Wu, Z., Foufoula-Georgiou, E., Parker, G., Singh, A., Fu, X., & Wang, G. (2019). Analytical solution for anomalous diffusion of bedload tracers gradually undergoing burial. *Journal of Geophysical Research: Earth Surface*, *124*. https://doi.org/10.1029/2018JF004654

Received 21 FEB 2018
Accepted 30 NOV 2018
Accepted article online 5 DEC 2018

Abstract Accounting for the burial of tracer particles during bedload transport is an important component in the formulation of tracer dispersal in rivers. Herein we propose a modified active layer formulation, which accounts for the effect of burial and admits analytical solutions, enabling insightful exploration of the phenomenon of superdiffusion of bedload tracers at the intermediate timescale. This phenomenon has been observed in recent numerical results using the 2-D Exner-Based Master Equation. By assuming that tracers in the active layer can exchange with nontracer particles in the substrate layer to preserve mass, and that tracers entering the substrate layer get permanently trapped during the timescale of analysis, we are able to deduce governing equations for the tracer concentration in both layers. The active layer tracer concentration is shown to be governed by an advection-diffusion equation with a sink term, and the increase of tracers in the substrate layer is driven by a corresponding source term. The solution for the variance of tracer population is analytically determined and can be approximated by the sum of a diffusion-induced scaling ($\propto t^1$) and an advection-induced scaling ($\propto t^3$) terms at the intermediate timescale, which explains the phenomenon of superdiffusion. The proposed formulation is shown to be able to capture the key characteristics of tracer transport as inferred by comparison with available results of numerical simulations.

1. Introduction

Deployment of tracer particles to explore the transport, erosion, and deposition of bedload material has been extensively conducted in the course of laboratory and field experiments recently. Such deployments can provide essential information on the role of bedload transport with regard to aquatic life and water quality, for example, through the interactions of physical, chemical, and biological processes with dissolved contaminants, sediment particles, and aquatic habitat (Ferguson & Hoey, 2002; Hassan et al., 1991, 2013; Martin et al., 2012; Ng & Yip, 2001; Schwendel et al., 2011; Singh et al., 2009; Wong et al., 2007). Typical field studies seed tracer particles at different positions along the river (e.g., Ferguson et al., 2002), and the virtual velocity and dispersion of the entire tracer population can be computed by recording the streamwise travel distances of these tracers at a range of timescales. The theoretical basis of such explorations can be dated back to the classical work of Einstein (1950), who proposed a statistical description of bedload transport. The motion of bedload particles was formulated as a series of alternating steps and waiting periods, which were further quantified in terms of statistics (Einstein, 1937, 1950). This formulation has been widely followed and further developed (Ancey et al., 2008; Charru et al., 2004; Cheng & Chiew, 1998; Furbish et al., 2012; Ganti et al., 2010; Hassan et al., 1991; Hill et al., 2010; Nelson et al., 1995; Paintal, 1971; Parker et al., 2000; Pelosi et al., 2014; Singh et al., 2009; Tsujimoto, 1978).

The gradual separation of bedload tracer particles from each other during the transport process, which we term as "diffusion", can be mathematically characterized (Bouchaud & Georges, 1990; Metzler & Klafter, 2000) by the scaling of the variance σ^2 of the displacement of the ensemble of particles as a function of time t, that is, as $\sigma^2 \propto t^\gamma$, where γ is a constant. Transport processes that are governed by a diffusion equation (e.g., a Brownian motion) whose fundamental solution is a Gaussian distribution with variance growing linearly with

time ($\gamma = 1$) are referred to as normal diffusion. If $\gamma \neq 1$, which means that particles in the ensemble separate from each other at a rate either faster or slower than a normal diffusion process, the bedload transport is regarded as *anomalous*, specifically, superdiffusion ($\gamma > 1$; with a special case of $\gamma = 2$, ballistic diffusion) or subdiffusion ($\gamma < 1$).

Einstein's formulation suggests a normal diffusion regime for the transport of bedload particles; this is understood by the assumption of thin-tailed step length and waiting time distributions (Ganti et al., 2010; Schumer et al., 2009). However, there have been both experimental and field observations (Bradley et al., 2010; Drake et al., 1988; Martin et al., 2012; Nikora et al., 2002; Roseberry et al., 2012) confirming various anomalous diffusion regimes during bedload transport. Supported by disparate data sets, a conceptual model has been proposed (Nikora et al., 2002) for transitions from ballistic to normal and finally to subdiffusion as characterized by different timescales, qualitatively taking into account the effects of particle inertia, infinite resting periods, and other system properties for explaining the underlying mechanisms (Martin et al., 2012; Nikora et al., 2002). It has been argued that particle size heterogeneity, that is, a broad distribution of particle sizes, is a possible reason for anomalous diffusion (Ganti et al., 2010). This was theoretically interpreted as the superposition of thin-tailed (exponential) step length distributions for each particle size leading to a heavy-tailed form of the distribution (power law; e.g., Hill et al., 2010). Suggesting that heavy-tailed step length and/or waiting time distributions can be the cause of anomalous diffusion, fractional advection-diffusion equations have been introduced and applied in the mathematical formulation of bedload tracer transport (Bradley et al., 2010; Ganti et al., 2010; Pelosi et al., 2016; Schumer et al., 2009; Voller & Paola, 2010). Following these leads, a number of authors have directly focused on the waiting time distribution for bedload particles, for example, using sonar- and lidar-tracked bed elevation to calculate waiting times at each elevation level in flume experiments (Voepel et al., 2013) and modeling bed evolution by the mean-reverting random walk process (Martin et al., 2014).

All the abovementioned research is focused on explaining the emergence of anomalous diffusion in the context of heavy-tailed step length/or waiting time distributions, the theoretical basis of which can be credited to the systematic exploration of Weeks et al. (1996) on the biased random walk model. However, we note that the approach of attributing the various anomalous diffusion regimes to different combinations of heavy or thin tailed distributions (of step lengths and waiting times) is valid only for long-term asymptotic processes (Weeks et al., 1996). Thus, the mechanism of anomalous diffusion of bedload transport before this limit is reached remains unclear. It can be a challenge to distinguish the associated physical timescales for a specific process (Martin et al., 2012; Phillips et al., 2013). One interesting example in this respect that we can consider is the numerical simulation of Pelosi et al. (2016) revealing a streamwise superdiffusion of tracer particles within the time span of ~10^2 hr. The purpose of their study is to model the phenomenon of *advective slowdown* observed in field experiments (Ferguson et al., 2002; Ferguson & Hoey, 2002; Haschenburger, 2013), which characterizes the gradual decrease of mean values of streamwise virtual velocity (traveled distance divided by the flow duration) of the tracer population. The long-term asymptotic transport of tracer particles for such a system is indicated by the approach to a constant virtual velocity (Ferguson & Hoey, 2002), which is not reached in the results of Pelosi et al. (2016); thus it may not be appropriate to resort to the *tail characteristics* (of waiting time distribution) for interpretation of the emergent superdiffusion of the tracers.

Conversely, the physical process of gradual burial of tracer particles is key to the observed advective slowdown of bedload transport (Ferguson et al., 2002) and might also be responsible for the superdiffusion observed in numerical simulations (Pelosi et al., 2016). Basically, during bedload transport a moving particle can be deposited when it gets trapped in a *hole* associated with the microstructure of the riverbed surface and then may (a) be buried due to the deposition of bedload particles on top of it as well as in adjacent locations, or alternatively (b) be re-entrained into motion due to scour at an appropriate depth. The deeper the tracer particle gets buried, the harder it is to be re-entrained and to participate again in streamwise transport, thus affecting dispersion of the tracer population. Based on the 2-D Exner-Based Master Equation (2-D EBME; Pelosi et al., 2014), Pelosi et al. (2016) consider different probabilities for a particle to jump downstream at different vertical positions in the riverbed, so taking into account the effect of vertical exchange of particles (i.e., both burial and exhumation of particles) during streamwise transport. However, the 2-D EBME has to be solved numerically, a feature which limits the potential of obtaining physical insight into bedload transport (e.g., revealing the mechanism of intermediate timescale superdiffusion). As a comparison, analytical considerations are possible for the most simplified active layer formulation (Ganti et al., 2010; Parker et al., 2000).

Here the *active layer formulation* is used for the approach of EBME based on the concept of an active layer, which is a thin layer on top of the riverbed where bed material exchanges with bedload, which can be further characterized as a *dynamical active layer* associated with a characteristic length scale of bedload grain size (Church & Haschenburger, 2017). Under steady and uniform transport conditions, an advection-diffusion equation (ADE) has been deduced governing the streamwise transport of tracers in the active layer (Ganti et al., 2010), which however is incapable of capturing the key features of advective slowdown and superdiffusion, at least in the case of uniform sediment (Pelosi et al., 2016). This is due to the oversimplification of the active layer formulation by discarding any vertical structure within the active layer, and neglecting particle exchange with the substrate layer underneath (Ganti et al., 2010; Parker et al., 2000; Pelosi et al., 2014). We expect that a formulation accounting for a simplified version of vertical exchange of tracers between the active layer and the substrate would enable an insightful theoretical study regarding bedload transport at the intermediate timescale.

To this end, in this paper we explicitly incorporate the process of gradual burial of tracer particles into the active layer formulation for bedload transport, enabling a convenient analytical treatment of the burial effect. In section 2, we present a new formulation and use it to deduce the governing equations for tracer particle concentration distributions in both the active and substrate layers. Then we solve the governing equations to obtain detailed information about transport processes in each layer and also the total concentration distribution for the whole tracer population. In section 3, we analytically obtain the moments of the concentration probability density function, and in particular the time evolution of the variance of the tracer population. This dependence of variance on time allows the determination of the different anomalous regimes of bedload diffusion that may arise. Through comparison with existing numerical results, we demonstrate that even this simplified model that admits analytical solutions can well capture the key characteristics of the tracer particle transport in terms of the advective slowdown and superdiffusion features. The limitations and strengths of the present model are discussed in the last subsection.

2. Formulation

2.1. Shallow Burial and Exhumation of Particles in the Active Layer Formulation

In the original active layer formulation (Ganti et al., 2010; Parker et al., 2000; Pelosi et al., 2014), it is assumed that only a thin top layer (the active layer, with a thickness L_a [L]) of the bed material can exchange with the moving bedload particles through entrainment (measured by E, the mean volume rate per unit area of particles entrained into transport [L/T]) and deposition (measured by D, the mean volume rate per unit area at which particles cease motion and enter the active layer [L/T]). Below the active layer, there is a so-called substrate layer with a thickness of L_s, the material of which does not exchange with the active layer (no net aggradation or degradation under the equilibrium transport conditions). Thus, what is described by the active layer formulation for the transport of a single tracer particle is as follows. The tracer may initiate its transport from this top layer of riverbed, the active layer, by performing a *jump* (*entrainment* into flow) with a random length to a downstream location (*deposition* back into active layer) and temporarily staying there, until it starts the next *jump* after a random time interval (waiting time). This process is characterized by the jump length and waiting time distributions of the tracer particles, which are in turn related to the physical transport environment, including flow conditions and particle size. We note that physically, a tracer should stay on top of the riverbed at the very beginning of the waiting period, but it can be buried by other particles arrived at some later time (burial), before it is entrained to move again (exhumation). It is seen that by specifying this one-dimensional (streamwise) travel-and-stop behavior of tracers in the active layer, the relatively frequent burial and exhumation of particles (i.e., at a relatively short timescale characterized by a couple of successive *jumps* and *waiting periods* of a tracer) in a shallow layer of the riverbed during streamwise transport can be analyzed.

2.2. Deep Burial of a Small Portion of Particles

In contrast to the relatively frequent vertical exchange of tracers in a shallow upper layer of the riverbed adjacent to flowing water, during longer times of transport consisting of many successive *jumps* and *waiting periods* of a particle, the ensemble of tracers can gradually move deeper and deeper downward into the bed, which may cause a very small portion of the particles to be buried deep enough to become effectively immobile for later transport (at the timescale of consideration). Such behavior has been found in field measurements (Ferguson et al., 2002; Hassan & Church, 1994). In this paper, to model this deep burial and

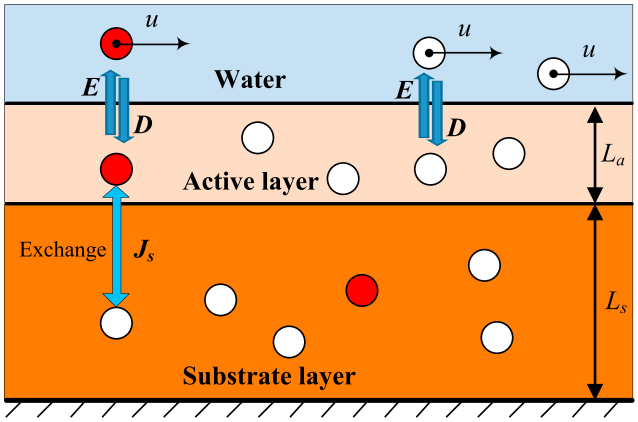

Figure 1. Schematic of the formulation of a riverbed with bedload particles moving in the water, an active layer that exchanges with the moving bedload particles, and a substrate layer of material. In this paper, the tracers (red circles) in the active layer can be entrained (with a volume rate per unit area per unit time E) into motion and deposited (with a volume rate per unit area per unit time D) somewhere downstream back into the active layer, or alternatively, become *permanently trapped* (characterized by a frequency J_s), at the middle-range timescales considered here, in the substrate layer.

near-immobilization of tracer particles during the bedload transport process, but at the same time maintain mass balance, we modify the active layer formulation and assume that there is an even exchange of tracer particles (from the active layer) with nontracer particles (from the substrate layer) at a frequency J_s [1/T] (Figure 1, and $J_s \ll D$ for the deep burial), such that the thickness of both layers remains constant. The assumption could be justified in terms of negligible upward movement of deeply buried tracers from the substrate to the active layer, due to the facts that (1) deep burial of tracers is a very slow process ($J_s \ll D$) and (2) the number of tracer particles in the substrate is orders of magnitude smaller than that of nontracer particles, which may be roughly related to the fact that $L_a \ll L_s$ with L_a/L_s of the order of 10^{-2} (Hassan & Church, 1994). Under this assumption of our simplified formulation, once the tracer particles enter the substrate layer, they become permanently trapped and cannot be entrained into transport again, at least during the timescale of consideration. However, we note that this assumption provides a first estimate of the actual vertical exchange of bedload particles; deeply buried tracers may still move upward and participate again in the streamwise transport, although at a much smaller probability compared with that for deep burial. Furthermore, we emphasize that our approach mimics a pseudopermanent or quasipermanent trapping, in that particles in the substrate may be exhumed and re-entrained at large timescales. Using our simplification of *permanent trapping*, we can see how (and to what extent) the resulting model can reproduce the actual bedload transport in terms of capturing the key features of advective slowdown and superdiffusion for the ensemble of tracer particles at intermediate timescales.

We start from the classical entrainment form of the Exner equation of sediment conservation (Ganti et al., 2010; Parker et al., 2000; Pelosi et al., 2014):

$$\left(1-\lambda_p\right)\frac{\partial \eta(x,t)}{\partial t} = -E(x,t) + D(x,t), \tag{1}$$

where λ_p is the bed porosity, η is the mean bed elevation [L], and t is the time [T]. Following Pelosi et al. (2014), we introduce the particle entrainment frequency J [1/T] in the definition of the sediment entrainment rate:

$$E(x,t) = \left(1-\lambda_p\right)D_p J(x,t), \tag{2}$$

where D_p is particle size [L]. We also relate the deposition rate at point x to the entrainment rates upstream in terms of the following convolution integral (Ganti et al., 2010; Parker et al., 2000):

$$D(x,t) = \int_0^\infty E(x-r,t)p_s(r)\mathrm{d}r, \tag{3}$$

where $p_s(r)$ is the probability density function (PDF) of step length. Neglecting the travel time of particle step during transport, equation (3) accounts for deposited particles at a given streamwise location coming from all the upstream locations, with a specific step length for each particle equal to the distance between its entrainment and deposition. We then rewrite equation (1) in the form

$$\frac{\partial \eta(x,t)}{\partial t} = -D_\mathrm{p} J(x,t) + D_\mathrm{p} \int_0^\infty J(x-r,t)p_s(r)\mathrm{d}r. \tag{4}$$

We denote by f_a the fraction of tracer particles in the active layer. Considering the simplified case of equilibrium transport, for which η, L_a, J, and the PDF of $p_s(r)$ are all constant with respect to time t and streamwise position x, the active layer formulation (equation (4)) without considering the burial effect is

$$L_\mathrm{a}\frac{\partial f_\mathrm{a}(x,t)}{\partial t} = -D_\mathrm{p} J\, f_\mathrm{a}(x,t) + D_\mathrm{p} \int_0^\infty J\, f_\mathrm{a}(x-r,t)p_s(r)\mathrm{d}r, \tag{5}$$

which indicates the conservation of tracer particles in the active layer. Thus, the time variation of tracers (the term in the LHS of equation (5)) is caused by the combined action of entrainment (tracers leaving the active layer, the first term in the RHS of equation (5)) and deposition (tracers entering the active layer, the second term in the RHS of equation (5)).

Particle burial basically corresponds to another process under which the tracers leave the active layer at rate J_s, which is here taken as a constant, indicating a constant fraction of active layer tracers that are removed per unit time. When considered in the governing equation, the term to account for the burial effect is similar in form with that for entrainment:

$$L_\mathrm{a}\frac{\partial f_\mathrm{a}(x,t)}{\partial t} = -D_\mathrm{p} J\, f_\mathrm{a}(x,t) - D_\mathrm{p} J_s f_\mathrm{a}(x,t) + D_\mathrm{p} J \int_0^\infty f_\mathrm{a}(x-r,t)p_s(r)\mathrm{d}r. \tag{6}$$

Correspondingly, tracers leaving the active layer enter the substrate layer as a result of the burial effect, leading to an increase of the fraction of tracer particles f_s in the substrate layer:

$$L_s\frac{\partial f_s(x,t)}{\partial t} = D_\mathrm{p} J_s f_\mathrm{a}(x,t), \tag{7}$$

where the constant L_s is the thickness of the substrate layer.

Proceeding under the assumption of a thin-tailed step length distribution, we apply the Fourier transform (Ganti et al., 2010; Pelosi et al., 2016)

$$\bar{f}_\mathrm{a}(k,t) = \int_{-\infty}^\infty \exp(-\mathrm{i}kx) f_\mathrm{a}(x,t)dx \tag{8}$$

to equation (6), obtaining

$$L_\mathrm{a}\frac{\partial \bar{f}_\mathrm{a}(k,t)}{\partial t} = -D_\mathrm{p} J\ \bar{f}_\mathrm{a}(k,t) + D_\mathrm{p} J\ \bar{f}_\mathrm{a}(k,t)\hat{p}_s(k) - D_\mathrm{p} J_s\ \bar{f}_\mathrm{a}(k,t), \tag{9}$$

We then introduce a Taylor series expansion for the transformed step length PDF, keeping only the first three terms:

$$\hat{p}_s(k) = 1 - \mathrm{i}k\mu_1 + \frac{1}{2}(ik)^2\mu_2 + \cdots, \tag{10}$$

where

$$\mu_p = \int_{-\infty}^{\infty} r^p p_s(r) dr \tag{11}$$

is the pth order moment of the step length PDF.

Substituting equation (10) into equation (9) and performing an inverse Fourier transform leads to an ADE (with sink term) for tracers in the active layer:

$$\frac{\partial f_a(x,t)}{\partial t} = -c\frac{\partial f_a(x,t)}{\partial x} + D_d\frac{\partial^2 f_a(x,t)}{\partial x^2} - \chi f_a(x,t), \tag{12}$$

and a corresponding result for tracers in the substrate layer (from equation (7)):

$$\frac{L_s}{L_a}\frac{\partial f_s(x,t)}{\partial t} = \chi f_a(x,t), \tag{13}$$

where

$$c = \frac{D_p J \mu_1}{L_a}, \quad D_d = \frac{D_p J \mu_2}{2L_a}, \quad \chi = \frac{D_p J_s}{L_a}. \tag{14}$$

Here c is the virtual velocity by which the centroid of the tracer population in the active layer travels downstream, D_d is the diffusion coefficient characterizing the diffusion of the tracer population in the active layer, and χ is the scaled burial frequency [1/T] (constant fraction of active layer tracers that are removed per unit time).

Note that equations (12) and (13) are all linear equations, so we can define the nondimensionalized bedload tracer concentrations in the active and substrate layers, respectively, as

$$C_a(x,t) = \frac{L_a f_a(x,t)}{M}, \quad C_s(x,t) = \frac{L_s f_s(x,t)}{M}, \tag{15}$$

where $M = \int_{-\infty}^{+\infty} [L_a f_a(x,t) + L_s f_s(x,t)]\, dx$ is determined by the initially released ($t = 0$) total amount of tracer particles, which does not change with time (thus a constant) due to conservation of tracers in the system. This leads to the governing equations

$$\frac{\partial C_a(x,t)}{\partial t} = -c\frac{\partial C_a(x,t)}{\partial x} + D_d\frac{\partial^2 C_a(x,t)}{\partial x^2} - \chi C_a(x,t), \tag{16}$$

and

$$\frac{\partial C_s(x,t)}{\partial t} = \chi C_a(x,t), \tag{17}$$

with the total dimensionless tracer concentration being

$$C_{tot}(x,t) = C_a(x,t) + C_s(x,t). \tag{18}$$

Compared with the ADE for bedload tracers derived by Ganti et al. (2010), it is seen in equation (16) that an additional sink term is present in the governing equation for tracer particle concentration within the active layer, indicating a gradual decrease of tracer mass remaining in this layer as time passes. Equation (16) is consistent in form with the result deduced under the framework of birth-death Markov processes for active bedload particles (Ancey et al., 2015; Ancey & Heyman, 2014), the exchange of which with nonactive particles by entrainment and deposition is represented by a source term in the governing equation (the source term here captures both burial and exhumation of particles). In comparison, the sink term in equation (16) represents a simplified process (only the burial effect for active tracers), which can be seen as a *permanent sink* for tracers during the timescale under consideration.

3. Results and Discussion

When focusing on the transport process of bedload tracers, not only must the active tracer particles in the active layer be considered, but also the tracer particles trapped in the substrate layer should be accounted for (Ganti et al., 2010; Parker et al., 2000; Pelosi et al., 2014). Thus, the discussion here with regard to tracer concentration distribution and its variance will be based on total concentration, as defined by equation (18).

3.1. Particle Concentration Distribution and Evolution

The technique of exponential transformation is a standard method for solving the ADE with a sink term like equation (16) (Ancey & Heyman, 2014; Zeng & Chen, 2011). Here we rewrite the active-layer tracer concentration $C_a(x, t)$ into the form of a product involving an exponential term:

$$C_a(x,t) = C_a^{'}(x,t)\exp(-\chi\, t), \tag{19}$$

which can be used to eliminate the sink term in equation (16) with $C_a^{'}(x, t)$, as well as the scaled burial frequency χ is defined in equation (14). Substituting equation (19) into equation (16) yields

$$\frac{\partial C_a^{'}(x,t)}{\partial t} = -c\frac{\partial C_a^{'}(x,t)}{\partial x} + D_d\frac{\partial^2 C_a^{'}(x,t)}{\partial x^2}, \tag{20}$$

which turns out to be a conventional ADE.

Consider the case for which all the tracer particles are released within the active layer of the riverbed at the very beginning of the observation period ($t = 0$) at the origin ($x = 0$). Then, the initial condition is a Dirac delta function for the active layer:

$$\begin{aligned} C_a(x,t)|_{t=0} &= \delta(x), \\ C_s(x,t)|_{t=0} &= 0. \end{aligned} \tag{21}$$

Under the given initial condition, equation (20) can be easily solved to give

$$C_a^{'}(x,t) = \frac{1}{\sqrt{4\pi D_d\, t}}\exp\left(-\frac{(x-ct)^2}{4D_d\, t}\right), \tag{22}$$

and the tracer concentration distribution in the active layer is obtained from equation (19) as

$$C_a(x,t) = \frac{1}{\sqrt{4\pi D_d\, t}}\exp\left(-\frac{(x-ct)^2}{4D_d\, t} - \chi\, t\right). \tag{23}$$

Based on equations (17), (18), and (23), we obtain

$$\begin{aligned} C_{tot}(x,t) = {} & \frac{1}{\sqrt{4\pi D_d\, t}}\exp\left(-\frac{(x-ct)^2}{4D_d\, t} - \chi\, t\right) \\ & + \int_0^t \frac{\chi}{\sqrt{4\pi D_d\, t}}\exp\left(-\frac{(x-ct)^2}{4D_d\, t} - \chi\, t\right)\mathrm{d}t. \end{aligned} \tag{24}$$

Equation (22) is the solution for the conventional ADE, indicating that at a given time, the streamwise distribution of the tracer concentration forms a Gaussian distribution. As time passes, the center of the Gaussian distribution moves downstream with virtual velocity c, while the spreading of the distribution is characterized by the diffusion coefficient D_d. With the burial effect incorporated, the evolution of the tracer concentration in the active layer is additionally affected by an exponential decay term (see equation (23)). As shown in Figure 2, compared with the distributions in the absence of the burial effect, the total mass of tracer particles in the active layer (i.e., the area under the curve) gradually decreases. In addition, the area difference between each pair of curves at a given time represents the tracer mass trapped in the

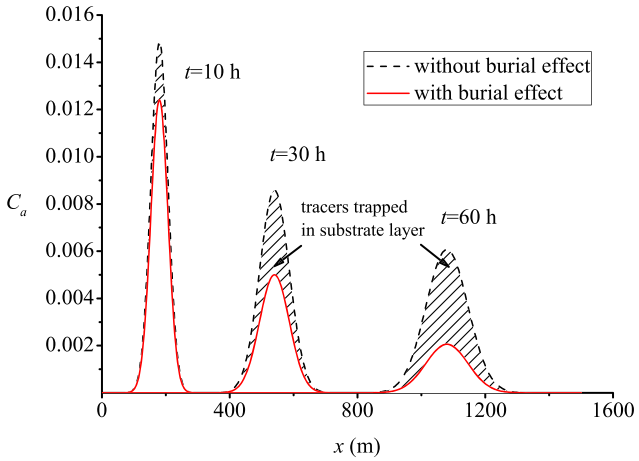

Figure 2. Spatial distribution of the active-layer tracer concentration (C_a) at three different times: with (red solid line, characterized by equation (23)) and without (black dashed line) the effect of permanent burial of tracers in the substrate layer. The parameters chosen to show the evolution are as follows: $D_d = 0.01$ m^2/s, $c = 0.005$ m/s, $\chi = 5 \times 10^{-6}$ s^{-1}.

substrate layer. The concentration distribution of tracer particles in the substrate layer is determined by the second term in the RHS of equation (24), which also reflects the fact that nontracer particles in the substrate layer move into the active layer (mass conservation for each layer). The integral cannot be expressed in explicit form, but it can be easily evaluated numerically.

The total concentration distribution is obtained by accounting for tracer particles in both the active and substrate layers, as specified by equation (24) and illustrated in Figure 3. It is obvious that immobile tracers buried in the substrate layer introduce an upstream tail in the concentration distribution, and the downstream peak of the distribution corresponds to the central location of the tracers within the active layer. Also, since the buried tracers in the substrate layer are immobile, the shape of the upstream tail remains invariant, in comparison with the peak of the concentration distribution traveling downstream at constant velocity c.

3.2. Analytical Solution for Tracer Concentration Variance

Since we have already obtained the total concentration distribution describing the bedload tracer particles transported as a virtual plume (equation (24)), we can now directly calculate the variance of the distribution to distinguish different regimes of bedload diffusion. We do this as an alternative to resorting to the Einstein-Smoluchowski description (Fathel et al., 2016), which requires information on the trajectories of the particles. In order to obtain the analytical solution for the variance of the bedload tracer concentration, we first define the pth order concentration moment

$$m_p(t) = \int_{-\infty}^{\infty} x^p C_{tot}(x,t)\mathrm{d}x. \tag{25}$$

The relation between the variance and the moments can be expressed as

$$\sigma^2(t) = \int_{-\infty}^{\infty} (x - m_1)^2 C_{tot}(x,t)\mathrm{d}x = m_2 - m_1^2. \tag{26}$$

We can easily calculate the first three concentration moments m_0, m_1 and m_2 by substituting equation (24) into equation (25):

$$m_0 = 1, \tag{27}$$

$$m_1(t) = \frac{c}{\chi}(1 - \mathrm{e}^{-\chi t}), \tag{28}$$

and

$$m_2(t) = \frac{2D_d(1 - \mathrm{e}^{-\chi t})}{\chi} + \frac{2(1 - \mathrm{e}^{-\chi t} - \mathrm{e}^{-\chi t}\chi t)c^2}{\chi^2}. \tag{29}$$

The zeroth-order concentration moment m_0 stands for the normalized total mass of bedload tracers in the river. As expected from the mass conservation of tracers, $m_0 = 1$; that is, the initially released tracers either stay in the active layer and gradually travel downstream, or become permanently buried somewhere (in x direction) in the substrate layer and cannot be entrained anymore.

The first-order concentration moment m_1 describes the streamwise displacement of the centroid of the tracer particle population (or the mean travel distance of the virtual plume). If we calculate the downstream travel velocity of the centroid by

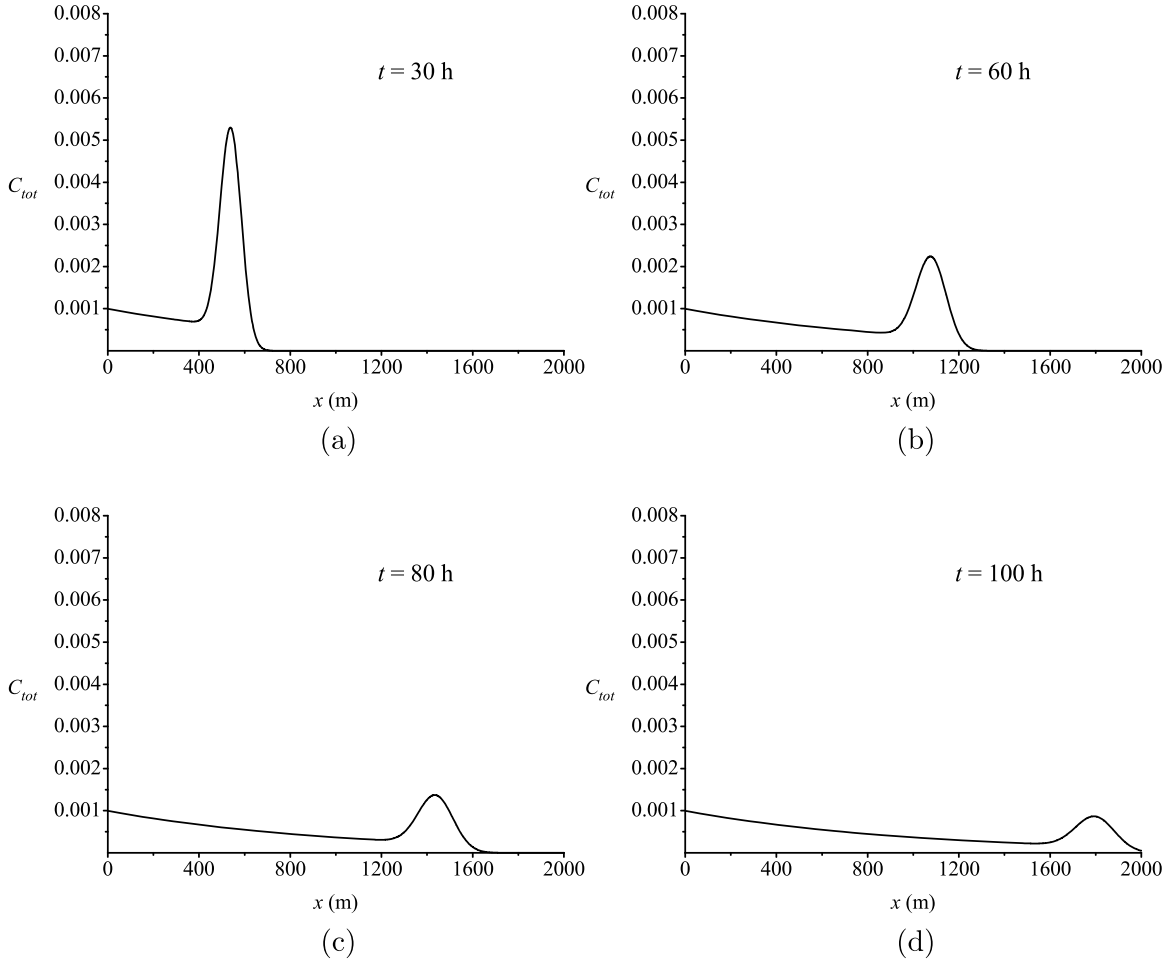

Figure 3. Spatial distribution of total (active layer + substrate, by equation (24)) concentration (C_{tot}) of tracer particles at different times. The parameters adopted are $D_d = 0.01$ m^2/s, $c = 0.005$ m/s, $\chi = 5 \times 10^{-6}$ s^{-1}, the same as those for Figure 2.

$$v = \frac{dm_1}{dt} = c\ e^{-t\chi}, \tag{30}$$

it is seen that when considering all the tracer particles, the velocity in equation (30) decreases with time, which agrees with the results of Pelosi et al. (2016) indicating an *advective slowdown* of the mean streamwise velocity of the tracer population. Although the centroid of the active tracers (tracers in the active layer) continues to move downstream at constant velocity c (Figure 2), the velocity for the whole population slows down because more and more particles become permanently trapped (Figure 3). Asymptotically all tracers get trapped in the substrate layer, so that v in equation (30) converges to zero for a large time, the scale of which is dependent on the parameter of the scaled burial frequency χ. For example, for the case $t = 3/\chi$, v drops to ~5% of its initial value, and v can be considered as asymptotically approaching zero when t is an order of magnitude greater than $1/\chi$ (~0.0045% of the initial value), that is, following the criterion $t \gg 1/\chi$.

Finally, we deduce the analytical solution for the variance of the tracer particle population according to equations (26)–(29):

$$\sigma^2(t) = \frac{2D_d(1 - e^{-\chi t})}{\chi} + \frac{(1 - e^{-\chi t} - 2e^{-\chi t}\chi t)c^2}{\chi^2}. \tag{31}$$

Understanding how $\sigma^2(t)$ evolves with time allows us to determine the diffusion regimes for the released bedload tracers during transport. In order to do this, it is useful to analyze the following two parts of the expression in the RHS of equation (31):

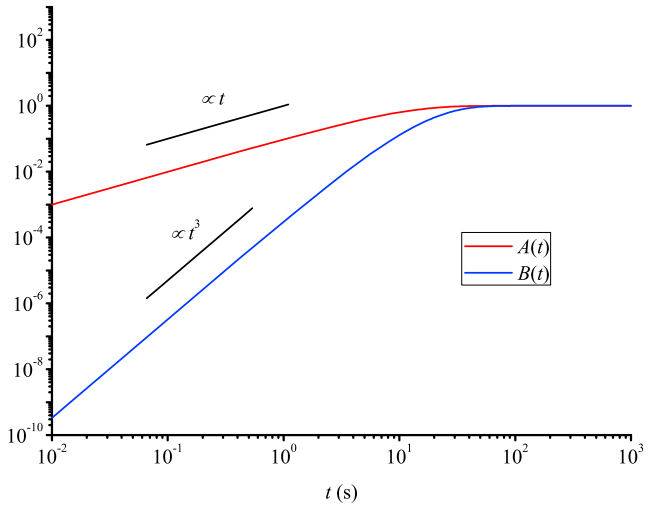

Figure 4. Evolution of the diffusion- and advection-induced scaling parameters $A(t)$ and $B(t)$, respectively (according to equations (32) and (33)) with time. The scaled burial frequency is $\chi = 0.1\ s^{-1}$. When t is an order of magnitude greater than $1/\chi$ (10^2 s in the figure), both $A(t)$ and $B(t)$ approach constants.

$$A(t) = 1 - e^{-\chi t} \tag{32}$$

and

$$B(t) = 1 - e^{-2\chi t} - 2e^{-\chi t}\chi t. \tag{33}$$

As a result of the exponential decay with time in equations (32) and (33), it is clear that after sufficiently long time ($t \gg 1/\chi$), both $A(t)$ and $B(t)$ approach constants. This means that there is no tracer dispersion because when all the particles have been buried, no tracer transport is possible. We expand equations (32) and (33) into a Taylor series to obtain information about their short-term behavior. Neglecting the higher-order terms, equations (32) and (33) simplify to

$$A(t) \approx \chi t, \tag{34}$$

and

$$B(t) \approx \frac{\chi^3 t^3}{3}. \tag{35}$$

According to the results, both $A(t)$ and $B(t)$ start evolving linearly in the log-log plots shown in Figure 4, although each has a different slope. Each curve gradually flattens out to a constant value at large t. Note from equations (31), (32), and (33) that $\sigma^2(t)$ is a linear combination of $A(t)$ and $B(t)$ and that for short-time evolution, $\sigma^2(t)$ scales as t, indicating a normal diffusion regime for the tracer particles. This is because at the very beginning, the fraction of trapped particles is so small that the *burial effect* can be neglected and the transport can be described by the conventional ADE without the sink term (Ganti et al., 2010). This formulation dictates a normal diffusion process.

It should be noted that there exists a *prenormal diffusion stage* (e.g., ballistic diffusion) before tracer transport can be governed by an ADE. This is mathematically revealed in Ganti et al. (2010) in the course of the deduction of the ADE, where the higher-order terms in the step length expansion are neglected, thus corresponding to a *long time* approximation for the process. This *long time* can be short in value for practical cases of bedload transport; for example, it can be of the order of only a few seconds (Fathel et al., 2015; Nikora et al., 2002) and so should be distinguished from the asymptotic timescale ($t \gg 1/\chi$) we mentioned previously for most of the tracers getting buried during transport. This *prenormal diffusion stage* is also qualitatively explained as an *inertial effect* (Martin et al., 2012; Nikora et al., 2002). Thus, the appearance of the short-time normal diffusion regime as discussed based on equation (34) depends on the value of the scaled burial frequency χ, which determines the time for the onset of the later anomalous diffusion regimes.

3.3. Diffusion Regimes for the Tracer Population

To further reveal the physical meaning of the two defined functions $A(t)$ and $B(t)$, we first substitute their short-term approximations (equations (34) and (35)) into equation (31):

$$\sigma^2(t) \approx 2D_d t + \frac{\chi c^2}{3} t^3, \tag{36}$$

which can be compared with the variance for the bedload transport described by the conventional ADE without the sink term (i.e., without burial effect):

$$\sigma^2_{ADE}(t) = 2D_d t. \tag{37}$$

Basically, the first term in the RHS of equation (36) is the same as that of equation (37), indicating the particle diffusion induced by the diffusion term of the ADE. For the case of equation (37), the advection effect does not cause particle diffusion because every particle virtually travels downstream at the same constant velocity c. However, considering that particles are getting buried, and thus their distances with

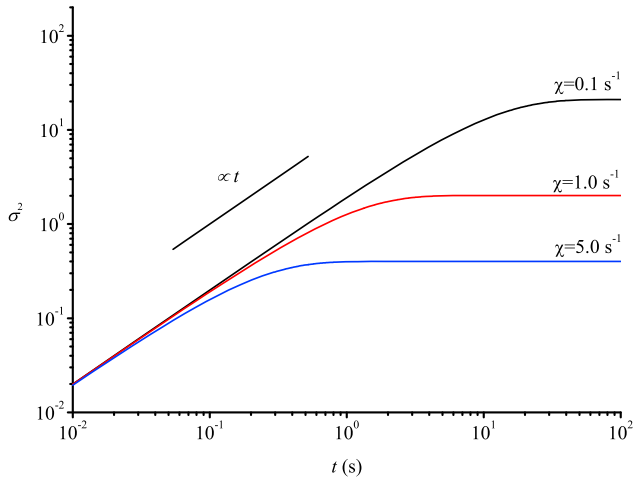

Figure 5. Variance of the bedload tracer concentration $\sigma^2(t)$ as a function of time (equation (38)) under the condition $D_{d\chi} \gg c^2$ (diffusion-dominated process) and for parameters D_d = 1 cm^2/s, c = 0.1 cm/s.

respect to the rest of the moving particles increase all the time, the case of equation (36) suggests a new mechanism of superdiffusion as revealed by the second term in the RHS of equation (36). Thus, physically, $A(t)$ is a diffusion-induced scaling ($\propto t^1$), and $B(t)$ is an advection-induced scaling ($\propto t^3$).

It should be noted that the term *burial effect* describes one of the physical processes of tracer transport. According to the above analysis, this physical process explains superdiffusion at intermediate timescales by the advection-induced scaling term, highlighting the accelerated streamwise dispersion of particles contributed by advective scattering among the group of traveling tracers and those trapped in the substrate. In explaining anomalous diffusion, the alternative approach of looking at the *tail characteristics* (Bradley, 2017; Phillips et al., 2013) only applies to asymptotic processes (i.e., $t \to \infty$; Weeks et al., 1996), and the timescale at which asymptotic behavior is reached can be difficult to determine for practical cases (Bradley, 2017; Martin et al., 2012). Additionally, it may be problematic when there exists a transition in the slope of the power law tail of the waiting time distribution (Voepel et al., 2013) as the observation period increases. Conversely, regarding field and laboratory experiments for studying anomalous diffusion of bedload transport, the identification and characterization of the tracer burial process (which can be related to advective slowdown according to equation (30)) may be easier to monitor as to directly quantify the form of the heavy-tailed waiting time distribution during tracer transport.

Again, because $\sigma^2(t)$ is a linear combination of $A(t)$ and $B(t)$,

$$\sigma^2(t) = \frac{1}{\chi^2}\left[2D_{d\chi}A(t) + c^2B(t)\right], \tag{38}$$

at an intermediate timescale before both $A(t)$ and $B(t)$ decay to constants ($t < 1/\chi$), the time evolution of $\sigma^2(t)$ is determined by the relative magnitude of the diffusion-induced term and the advection-induced term on the RHS of equation (38). This leads to a useful relation involving $D_{d\chi}$ and c^2 (the coefficients of $A(t)$ and $B(t)$ according to equation (38)).

One of the simplest cases would be such that either $D_{d\chi}$ or c^2 dominates, resulting in a scaling characterized by either $A(t)$ (the diffusion-induced scaling) or $B(t)$ (the advection-induced scaling). For example, if the process is diffusion-dominated, that is, $D_{d\chi} \gg c^2$, the second term at the RHS of equation (31) can be neglected and the diffusion regimes for the tracer particles during the transport become consistent with that of $A(t)$, as shown in Figure 5. With $\sigma^2(t)$ increasing linearly with time at an early stage, but with the rate of increase gradually decreasing to zero, we find in the log-log plot of Figure 5 a transition from normal diffusion to subdiffusion. Also in this figure we can see that as the scaled burial frequency χ decreases, the onset of the transition time is delayed, and the overall time for the transport increases, which agrees with the understanding that the slower the burial process, the longer the time needed to break the normal diffusion regime, and also to have an effect on the great majority of the tracer particles, which are initially concentrated in the active layer.

Conversely, if the process is advection-dominated, that is, $D_{d\chi} \ll c^2$, the first term at the RHS of equation (31) can be neglected and the diffusion regimes (both superdiffusion and subdiffusion) are dominated by $B(t)$, as shown in Figure 6. We note that there will always be a regime of normal diffusion when time is sufficiently short ($t \ll \sqrt{D_d}/c/\sqrt{\chi}$). This is because when the value of t decreases, the advection-induced scaling term ($\propto t^3$) can decrease much faster than the diffusion-induced scaling term ($\propto t^1$). After the initial normal diffusion stage, the regime gradually transforms to superdiffusion with the scaling of t^3 at the intermediate timescale ($\sqrt{D_d}/c/\sqrt{\chi} < t < 1/\chi$). Finally, at large timescales ($t \gg 1/\chi$), it will transform back to subdiffusion as the time-dependent terms in $\sigma^2(t)$ converge to zero.

In more complicated situations with $D_{d\chi}$ comparable to c^2, which means that each of the terms $A(t)$ and $B(t)$ plays an important role in the result, it is shown in Figure 7 that the evolution of the variance $\sigma^2(t)$ shares great

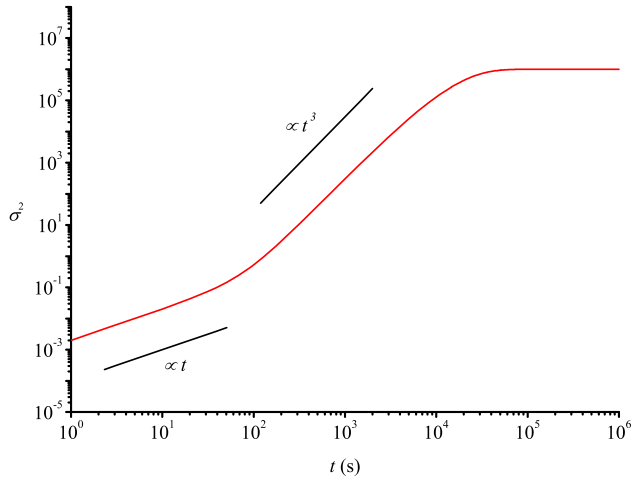

Figure 6. Variance of the bedload tracer concentration $\sigma^2(t)$ as a function of time (equation (38)) under the condition $D_d\chi \ll c^2$ (advection-dominated process) and for parameters D_d=10^{-3} cm^2/s, $\chi = 10^{-4}$ s^{-1}, c = 0.1 cm/s.

similarity with the superdiffusion case shown in Figure 6, except that the slope of the curves during the intermediate timescale can vary from 1 to 3, depending on the specific parameters. We summarize different diffusion regimes under different conditions in Table 1.

3.4. Comparison With Existing Numerical Results Based on Experimental Data

The 2-D EBME (by Pelosi et al., 2016) takes into account the fact that bedload particles buried deeper have a lower possibility to be entrained and accounts for not only streamwise but also vertical transport of tracers, representing a more complicated treatment compared with our simplified model in this paper. In order to examine how well the present approach can capture the key characteristics of the bedload transport process, in this section we compare the analytical solutions with existing numerical results of the 2-D EBME.

The experimental results of Wong et al. (2007) were used to determine the parameters needed for the numerical simulation (Pelosi et al., 2016). The uniform particle size is D_p = 7.1 mm, the jump frequency is J = 0.013 s^{-1}, and the PDF of step lengths is the exponential distribution

$$p_s(r) = \frac{1}{\langle r\rangle}\exp\left(-\frac{r}{\langle r\rangle}\right) \tag{39}$$

with the mean step length $\langle r\rangle$ = 1.08 m.

Based on equations (39) and (11), we obtain μ_1 = 1.08 m and μ_2 = 2.33 m^2. We also adopt the thickness of the active layer to be $L_a = 1.5D_p$ (Parker, 2008; Pelosi et al., 2016), so that by equation (14) we can calculate c = 0.009 m/s and D_d = 0.01 m^2/s.

The initial condition of the numerical simulation is a 50-m-long patch of tracer particles (Pelosi et al., 2016):

$$C_a(x,0) = \begin{cases} 1/50, & 0\,\mathrm{m} \le x \le 50\,\mathrm{m} \\ 0, & \text{elsewhere} \end{cases}, \tag{40}$$

which is different from what we considered in equation (21). Considering that the fundamental solution of equation (23) is for a *point-source* initial release of particles at x = 0, the corresponding solution for the initial release at an arbitrary streamwise location x_0 is given by

$$C_a(x,t,x_0) = \frac{1}{\sqrt{4\pi D_d\, t}}\exp\left(-\frac{(x-ct-x_0)^2}{4D_d\, t} - \chi\, t\right). \tag{41}$$

Thus, the total concentration distribution given the initial condition of equation (40) can be obtained as the integration of solutions under different *point-source* initial conditions:

$$C_{tot}(x,t) = \int_0^{50}\left[C_a(x,t,x_0) + \int_0^t \chi C_a(x,t,x_0)\mathrm{d}t\right]\mathrm{d}x_0. \tag{42}$$

Following again the procedure of obtaining the concentration moments and the variance based on equations (41) and (42), we have

$$m_0 = 1, \tag{43}$$

$$m_1 = 25 + \frac{c}{\chi}(1 - \mathrm{e}^{-\chi t}), \tag{44}$$

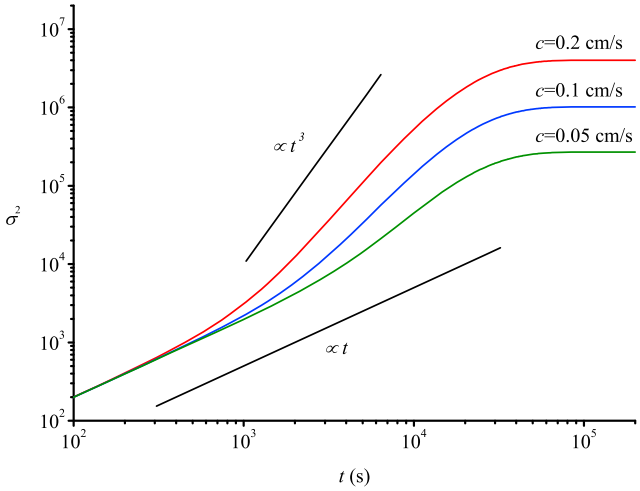

Figure 7. Variance of the bedload tracer concentration $\sigma^2(t)$ as a function of time (equation (38)) under the condition that both the diffusion-induced scaling $A(t)$ and the advection-induced scaling $B(t)$ play a role in the result and for parameters D_d = 1 cm^2/s, $\chi = 10^{-4}$ s^{-1}.

Table 1
Diffusion Regimes Under Different Conditions

Criterion	Short timescale $t \ll \sqrt{D_d}/c/\sqrt{\chi}$	Intermediate timescale $\sqrt{D_d}/c/\sqrt{\chi} < t < 1/\chi$	Large timescale $t \gg 1/\chi$
$D_d\chi \gg c^2$	Normal diffusion (neglect ballistic regime)	Normal diffusion	Subdiffusion (may deviate from reality due to the assumption of permanent burial)
$D_d\chi \sim c^2$		Superdiffusion ($\propto t^\gamma$, $\gamma \in (1,3)$)	
$D_d\chi \ll c^2$		Superdiffusion ($\propto t^3$)	

$$m_2 = \frac{2D_d(1-e^{-\chi t})}{\chi} + \frac{2c^2(1-e^{-\chi t}-e^{-\chi t}\chi t)}{\chi^2} + \frac{50c(1-e^{-\chi t})}{\chi} + \frac{2500}{3}, \tag{45}$$

and

$$\sigma^2(t) = m_2 - m_1^2 = \frac{2D_d(1-e^{-\chi t})}{\chi} + \frac{c^2(1-e^{-2\chi t}-2e^{-\chi t}\chi t)}{\chi^2} + \frac{625}{3}. \tag{46}$$

The first-order concentration moment m_1 characterizes the mean travel distance of the tracer population. It is obvious from equation (44) that the *advective slowdown* is mathematically characterized by an exponential decay process with the scaled burial frequency χ. This also provides a way to determine the parameter χ using numerical or experimental data. In Figure 8 we fit the numerically obtained mean travel distances to equation (44), demonstrating a key feature captured by the analytical treatment. It is seen that equation (44) better fits the numerical results than the power law relation Pelosi et al. (2016) applied. Using this fit we can obtain the parameters as $\chi = 3 \times 10^{-6}$ s^{-1} and $c = 0.006$ m/s, the latter of which agrees reasonably with the previously obtained value (0.009 m/s) calculated through equation (14) based on the experimental data.

In Figure 9 we show that the analytical approach can also capture the simulated anomalous diffusion regime. Based on the relation between $D_d\chi$ and c^2 that we suggested in section 3.3, the specific case considered here using the experimental data of Wong et al. (2007) agrees with the result of Figure 7, which indicates the existence of the intermediate timescale superdiffusion regime and the variance scaling as t^γ, where $\gamma \in (1,3)$.

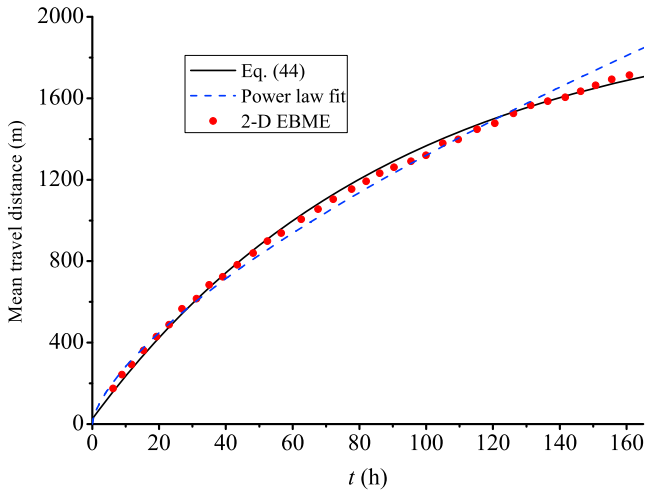

Figure 8. Mean travel distance as a function of time. A fit by equation (44) to the numerically obtained data by the 2-D Exner-Based Master Equation (2D-EBME) is used to determine the parameters $\chi = 3 \times 10^{-6}$ s^{-1} and $c = 0.006$ m/s. The results demonstrate that the analytical consideration captures well the advective slowdown of the tracer population. The power law fit (dashed line) by Pelosi et al. (2016) is also shown for reference.

Another interesting feature revealed by Figure 9 is the emergence of an initial subdiffusion regime, which was not discussed by Pelosi et al. (2016). Comparison between equations (46) and (31) shows the difference of a constant (625/3), introduced by the different initial condition of equation (40). Although having a negligible effect on the intermediate- and long-time scaling, this added constant changes the scaling of the variance at short times.

3.5. Limitations and Strengths of the Model

Based on the analysis presented in previous sections, we can see that the present model may be applied for bedload transport processes across a range of timescales depending on how quickly the tracer particles can be *permanently buried*. This speed is characterized by the key parameter χ, the information about which we need to extract from the physical system under investigation. The variety of timescales presented here is associated with distinct physical transport environments, and also relates to the processes under consideration. For example, in laboratory experiments, the process of interest can be as short as seconds (Fathel et al., 2015) or minutes (Martin et al., 2012): some traveling particles (sand or gravel) may be seen as *permanently buried* after one or two *jumps* because they will not be re-entrained in a short period at the timescale of consideration, although they may still rest on top of the bed. Conversely, long-term field measurements (Ferguson et al., 2002) of tracer pebbles in the

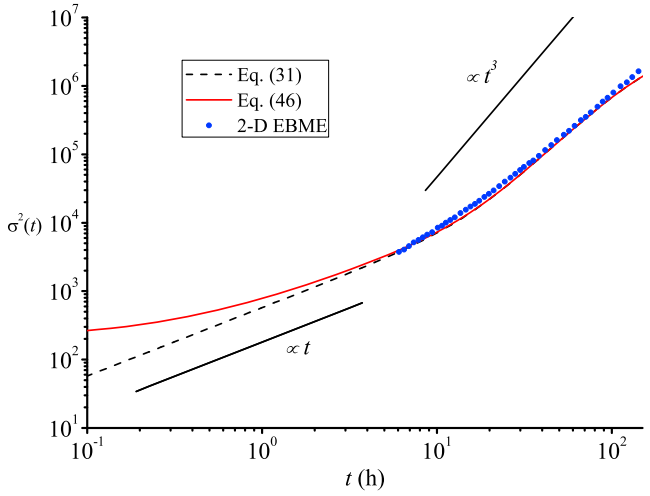

Figure 9. Variance of the bedload tracer concentration $\sigma^2(t)$ as a function of time. The analytical solution captures well the emergent superdiffusion regime obtained from numerical simulation of the 2-D Exner-Based Master Equation (2D-EBME) with parameters $\chi = 3 \times 10^{-6}$ s^{-1}, $c = 0.006$ m/s, and $D_d = 0.08$ m^2/s. A subdiffusion regime at short timescales (red line) is attributable to the initial condition of the numerical simulation of Pelosi et al. (2016; a 50-m-long patch of tracers), which is different from that used in this paper for equation (31) (a point-release of tracers at the origin of $x = 0$).

natural environment have focused on processes that last years, during which time the tracers were gradually buried ever deeper, with significant reduction of their mobility during the process. In either case, the re-entrainment of *permanently buried* tracers can be expected to start to play a role in streamwise transport as the observation period increases.

A major limitation of the present model is introduced by a key assumption of the formulation: deeply buried tracer particles cannot be re-entrained to participate again in streamwise transport. This may not be the case for large timescale transport of tracer particles (as discussed above). Thus, it is vital to first determine what this *large timescale* is for the specific bedload transport process, and then to see how well the model can perform at the corresponding *intermediate timescale*. According to section 3.2, this *large timescale* corresponds to when most of the tracers are *permanently buried* with almost no movement of the entire tracer population, and is mathematically characterized by $t \gg t_c = 1/\chi$. According to the results in section 3.4, we demonstrate that at the corresponding intermediate timescale ($t < 5\ t_c \sim 10^2$ hr for this case), the model can capture the key features of advective slowdown and superdiffusion.

The present model is based on the active layer formulation (Ganti et al., 2010; Pelosi et al., 2016) and is thus subject to corresponding idealized transport conditions (single particle size, mobile-bed equilibrium, temporally constant active layer thickness, etc.). However, instead of just revealing physical insights including the mechanism of superdiffusion (the merit of the theoretical analysis), it can also demonstrate its strength in application to the field process with a much more complicated transport environment. For example, for the tracer tracking field work done along Allt Dubhaig, a bar-riffle-pool headwater stream in Scotland, Ferguson et al. (2002) observed that the mean value of virtual velocity of the tracers during a period of 8.5 years can be ~40% slower compared with that of the first 2 years. Using this information alone and using equation (30) for the virtual velocity, we can approximate the parameter $\chi \approx 0.4$ year^{-1}. The result indicates a large timescale of $t > 5\ t_c \sim 10^1$ year for this specific process, which agrees with the time needed for the virtual velocity of the tracer population to approach a constant value (Ferguson & Hoey, 2002; Pelosi et al., 2016). Thus, the advective slowdown observed for this field case at the intermediate timescale ($t < 10^1$ year) can be described by the present model.

4. Conclusions

It has been observed in numerical simulations that the gradual burial of bedload tracer particles can cause superdiffusion during streamwise transport. The underlying mechanism for this anomalous diffusion process at intermediate timescales remains unclear because it may not be appropriate to refer to the tail characteristics of the waiting time distribution of tracers, which only applies to long-term asymptotic processes.

In this paper we have incorporated the particle burial effect into the active layer formulation by considering a constant frequency for tracer particles (from the active layer) to exchange with nontracer particles in the underlying substrate layer, where the tracers then get permanently trapped. This treatment introduces a simple vertical structure to distinguish between active and trapped tracer particles. It captures the mechanism of burial, while being sufficiently simple to enable an analytical study of the transport process. This is in contrast to the 2-D EBME approach previously applied by Pelosi et al. (2016), which must be solved numerically. However, we note that the assumption of permanent trapping is a first-order approximation of the vertical exchange of bedload particles in a riverbed, which may correspond to a major limitation of the resulting model in describing large timescale tracer transport.

In the governing equations obtained herein, the burial effect is represented by a sink term in the advection-diffusion equation (ADE) for tracers in the active layer, which also results in the increase of tracer particle concentration with time in the substrate layer. After solving the governing equations for the concentration

distribution, we have analytically deduced a relation for the variance of the tracer population based on concentration moments. According to its mathematical structure, we show that the variance is the sum of a diffusion-induced scaling ($\propto t^1$, governing the normal diffusion regime) and an advection-induced scaling ($\propto t^3$, governing the superdiffusion regime) for both short and intermediate timescale transport processes. It should be noted that the term *burial effect* characterizes a major physical process of tracer transport. When translated into our understanding of the source of anomalous diffusion, we note that for intermediate timescale superdiffusion, it is more appropriate to refer to the advection-induced scaling identified herein for accelerated streamwise dispersion associated with the coexistence of traveling particles and the remaining immobile tracers. The alternative approach of looking at the *tail characteristics* only applies to asymptotic processes (i.e., $t \to \infty$), and the timescale of reaching such asymptotic behavior can be difficult to determine for practical cases. In addition, it may be complicated when there exists a transition in the slope of the power law tail of the waiting time distribution as the observation period increases. Conversely, the identification and characterization of the tracer burial process may be easier to monitor and parameterize based on the analytical solution deduced in this paper. This solution captures the important feature of advective slowdown, which can be compared with direct attempts to characterize a heavy-tailed waiting time distribution based on field or laboratory experiments.

Compared to the single normal diffusion regime for bedload transport without considering loss of tracers from the active layer by burial, our results show the following:

1. There always exists a normal diffusion regime at short timescales ($t \ll \sqrt{D_d}/c/\sqrt{\chi}$, the case of no burial of particles).
2. There always exists a transition to a subdiffusion regime at sufficiently large timescales ($t \gg 1/\chi$), after most of the tracers get buried. However, this model is not applicable asymptotically, because it neglects the very small possibility that the deeply buried particles can still be re-entrained into streamwise transport. We note that it is important to first distinguish the applicable large timescale by the criterion $t \gg 1/\chi$. The relevant timescale for practical cases (i.e., application to natural rivers) can vary depending on the corresponding physical transport environment (section 3.5). The analytical solutions obtained in this paper work well before reaching the asymptotic limit (section 3.4).
3. At intermediate timescales, the appearance and characteristics of a superdiffusion regime depend on the relation between the product of the particle diffusion coefficient and the burial frequency, that is, $D_d\chi$, and the square of the virtual streamwise velocity c^2 for the tracer population.

(a) If $D_d\chi \gg c^2$, there will be no superdiffusion regime.
(b) If $D_d\chi \ll c^2$, there will be a superdiffusion regime with the variance scaling as t^3.
(c) If $D_d\chi$ is comparable to c^2, there will be a superdiffusion regime with the variance scaling as t^γ, where $\gamma \in (1, 3)$.

We have shown through comparison of the results between the obtained analytical solutions and the existing numerical simulation of Pelosi et al. (2016) using the 2-D EBME that the simplified formulation proposed herein can capture the key characteristics of bedload tracer transport in terms of appropriately revealing the features of advective slowdown and the superdiffusion regime. We also demonstrate how the analytical results obtained under idealized transport conditions can be extrapolated to a natural setting by adaptation to incorporate field processes in a much more complicated transport environment.

Notation

σ^2	bedload tracer concentration variance [L^2]
t	time [T]
L_a	active layer thickness [L]
L_s	substrate layer thickness [L]
λ_p	bed porosity [1]
η	mean bed elevation [L]
E	mean volume rate per unit area of bedload entrainment into transport [L/T]
D	mean volume rate of bedload deposition per unit area [L/T]
J	particle entrainment frequency [$1/T$]

J_s	burial frequency [1/*T*]
D_p	particle size [*L*]
x	streamwise coordinate [*L*]
$p_s(r)$	probability density function of step length [1/*L*]
f_a	fraction of tracer particles in the active layer [1]
f_l	fraction of tracer particles that exchange between active and substrate layers when aggradation and degradation occur [1]
f_s	fraction of tracer particles in the substrate layer [1]
μ_p	*p*th order moment of the step length probability density function [L^p]
c	virtual velocity [*L*/*T*]
D_d	particle diffusion coefficient [L^2/T]
χ	scaled burial frequency [1/*T*]
C_a	tracer concentration in active layer [1/*L*]
C_s	tracer concentration in substrate layer [1/*L*]
C_{tot}	total tracer concentration [1/*L*]
$\delta(x)$	Dirac delta function [1/*L*]
m_p	*p*th order moment of tracer concentration [L^p]
v	virtual velocity with advective slowdown [*L*/*T*]
$A(t)$	diffusion-induced scaling parameter [1]
$B(t)$	advection-induced scaling parameter [1]

Acknowledgments
This research was funded by NSF (grant EAR-1209402) under the Water Sustainability and Climate Program (WSC), NSF (grant EAR-1242458) under Science Across Virtual Institutes (SAVI), Natural Science Foundation of China (grants 51525901 and 51379100), and Tsinghua University Initiative Scientific Research Program (2014Z22066). We thank the Editor John M. Buffington, Associate Editor Christophe Ancey, and three anonymous reviewers whose constructive comments and suggestions improved our presentation and refined our interpretations. All the information for the theoretical analysis can be found in the text, and the data used are properly referenced.

References

Ancey, C., Bohorquez, P., & Heyman, J. (2015). Stochastic interpretation of the advection-diffusion equation and its relevance to bed load transport. *Journal of Geophysical Research: Earth Surface*, *120*, 2529–2551. https://doi.org/10.1002/2014JF003421

Ancey, C., Davison, A., Böhm, T., Jodeau, M., & Frey, P. (2008). Entrainment and motion of coarse particles in a shallow water stream down a steep slope. *Journal of Fluid Mechanics*, *595*, 83–114.

Ancey, C., & Heyman, J. (2014). A microstructural approach to bed load transport: Mean behaviour and fluctuations of particle transport rates. *Journal of Fluid Mechanics*, *744*, 129–168. https://doi.org/10.1017/jfm.2014.74

Bouchaud, J.-P., & Georges, A. (1990). Anomalous diffusion in disordered media: Statistical mechanisms, models and physical applications. *Physics Reports*, *195*(4–5), 127–293. https://doi.org/10.1016/0370-1573(90)90099-N

Bradley, D. N. (2017). Direct observation of heavy-tailed storage times of bed load tracer particles causing anomalous superdiffusion. *Geophysical Research Letters*, *44*, 227–235. https://doi.org/10.1002/2017GL075045

Bradley, D. N., Tucker, G. E., & Benson, D. A. (2010). Fractional dispersion in a sand bed river. *Journal of Geophysical Research*, *115*, F00A09. https://doi.org/10.1029/2009JF001268

Charru, F., Mouilleron, H., & Eiff, O. (2004). Erosion and deposition of particles on a bed sheared by a viscous flow. *Journal of Fluid Mechanics*, *519*, 55–80. https://doi.org/10.1017/S0022112004001028

Cheng, N.-S., & Chiew, Y.-M. (1998). Pickup probability for sediment entrainment. *Journal of Hydraulic Engineering*, *124*(2), 232–235. https://doi.org/10.1061/(ASCE)0733-9429(1998)124:2(232)

Church, M., & Haschenburger, J. K. (2017). What is the "active layer"? *Water Resources Research*, *53*, 5–10. https://doi.org/10.1002/2016WR019675

Drake, T. G., Shreve, R. L., Dietrich, W. E., Whiting, P. J., & Leopold, L. B. (1988). Bedload transport of fine gravel observed by motion-picture photography. *Journal of Fluid Mechanics*, *192*(1), 193–217. https://doi.org/10.1017/S0022112088001831

Einstein, H. (1937). Bedload transport as a probability problem. In *Sedimentation* (reprinted in 1972), (pp. 105–108). Colorado: Water Resources Publications.

Einstein, H. A. (1950). *The bed-load function for sediment transportation in open channel flows*. Washington, DC: US Department of Agriculture.

Fathel, S., Furbish, D., & Schmeeckle, M. (2016). Parsing anomalous versus normal diffusive behavior of bed load sediment particles. *Earth Surface Processes and Landforms*, *41*(12), 1797–1803. https://doi.org/10.1002/esp.3994

Fathel, S. L., Furbish, D. J., & Schmeeckle, M. W. (2015). Experimental evidence of statistical ensemble behavior in bed load sediment transport. *Journal of Geophysical Research: Earth Surface*, *120*, 2298–2317. https://doi.org/10.1002/2015JF003552

Ferguson, R., & Hoey, T. (2002). Long-term slowdown of river tracer pebbles: Generic models and implications for interpreting short-term tracer studies. *Water Resources Research*, *38*(8), 1142. https://doi.org/10.1029/2001WR000637

Ferguson, R. I., Bloomer, D. J., Hoey, T. B., & Werritty, A. (2002). Mobility of river tracer pebbles over different timescales. *Water Resources Research*, *38*(5), 1045. https://doi.org/10.1029/2001WR000254

Furbish, D. J., Haff, P. K., Roseberry, J. C., & Schmeeckle, M. W. (2012). A probabilistic description of the bed load sediment flux: 1. Theory. *Journal of Geophysical Research*, *117*, F03031. https://doi.org/10.1029/2012JF002352

Ganti, V., Meerschaert, M. M., Foufoula-Georgiou, E., Viparelli, E., & Parker, G. (2010). Normal and anomalous diffusion of gravel tracer particles in rivers. *Journal of Geophysical Research*, *115*, F00A12. https://doi.org/10.1029/2008JF001222

Haschenburger, J. (2013). Tracing river gravels: Insights into dispersion from a long-term field experiment. *Geomorphology*, *200*, 121–131. https://doi.org/10.1016/j.geomorph.2013.03.033

Hassan, M. A., & Church, M. (1994). Vertical mixing of coarse particles in gravel bed rivers: A kinematic model. *Water Resources Research*, *30*(4), 1173–1185. https://doi.org/10.1029/93WR03351

Hassan, M. A., Church, M., & Schick, A. P. (1991). Distance of movement of coarse particles in gravel bed streams. *Water Resources Research*, *27*(4), 503–511. https://doi.org/10.1029/90WR02762

Hassan, M. A., Voepel, H., Schumer, R., Parker, G., & Fraccarollo, L. (2013). Displacement characteristics of coarse fluvial bed sediment. *Journal of Geophysical Research: Earth Surface*, *118*, 155–165. https://doi.org/10.1029/2012JF002374

Hill, K. M., DellAngelo, L., & Meerschaert, M. M. (2010). Heavy-tailed travel distance in gravel bed transport: An exploratory enquiry. *Journal of Geophysical Research*, *115*, F00A14. https://doi.org/10.1029/2009JF001276

Martin, R. L., Jerolmack, D. J., & Schumer, R. (2012). The physical basis for anomalous diffusion in bed load transport. *Journal of Geophysical Research*, *117*, F01018. https://doi.org/10.1029/2011JF002075

Martin, R. L., Purohit, P. K., & Jerolmack, D. J. (2014). Sedimentary bed evolution as a mean-reverting random walk: Implications for tracer statistics. *Geophysical Research Letters*, *41*, 6152–6159. https://doi.org/10.1002/2014GL060525

Metzler, R., & Klafter, J. (2000). The random walk's guide to anomalous diffusion: A fractional dynamics approach. *Physics Reports*, *339*(1), 1–77. https://doi.org/10.1016/S0370-1573(00)00070-3

Nelson, J. M., Shreve, R. L., McLean, S. R., & Drake, T. G. (1995). Role of near-bed turbulence structure in bed load transport and bed form mechanics. *Water Resources Research*, *31*(8), 2071–2086. https://doi.org/10.1029/95WR00976

Ng, C. O., & Yip, T. L. (2001). Effects of kinetic sorptive exchange on solute transport in open-channel flow. *Journal of Fluid Mechanics*, *446*, 321–345.

Nikora, V., Habersack, H., Huber, T., & McEwan, I. (2002). On bed particle diffusion in gravel bed flows under weak bed load transport. *Water Resources Research*, *38*(6), 1081. https://doi.org/10.1029/2001WR000513

Paintal, A. (1971). A stochastic model of bed load transport. *Journal of Hydraulic Research*, *9*(4), 527–554. https://doi.org/10.1080/00221687109500371

Parker, G. (2008). Transport of gravel and sediment mixtures. In *Sedimentation engineering: Processes, measurements, modeling, and practice* (Vol. 110, pp. 165–252). Reston, VA: ASCE. https://doi.org/10.1061/9780784408148.ch03

Parker, G., Paola, C., & Leclair, S. (2000). Probabilistic Exner sediment continuity equation for mixtures with no active layer. *Journal of Hydraulic Engineering*, *126*(11), 818–826. https://doi.org/10.1061/(ASCE)0733-9429(2000)126:11(818)

Pelosi, A., Parker, G., Schumer, R., & Ma, H. B. (2014). Exner-Based Master Equation for transport and dispersion of river pebble tracers: Derivation, asymptotic forms, and quantification of nonlocal vertical dispersion. *Journal of Geophysical Research: Earth Surface*, *119*, 1818–1832. https://doi.org/10.1002/2014JF003130

Pelosi, A., Schumer, R., Parker, G., & Ferguson, R. (2016). The cause of advective slowdown of tracer pebbles in rivers: Implementation of Exner Based Master Equation for coevolving streamwise and vertical dispersion. *Journal of Geophysical Research: Earth Surface*, *121*, 623–637. https://doi.org/10.1002/2015JF003497

Phillips, C. B., Martin, R. L., & Jerolmack, D. J. (2013). Impulse framework for unsteady flows reveals superdiffusive bed load transport. *Geophysical Research Letters*, *40*, 1328–1333. https://doi.org/10.1002/grl.50323

Roseberry, J. C., Schmeeckle, M. W., & Furbish, D. J. (2012). A probabilistic description of the bed load sediment flux: 2. Particle activity and motions. *Journal of Geophysical Research*, *117*, F03032. https://doi.org/10.1029/2012JF002353

Schumer, R., Meerschaert, M. M., & Baeumer, B. (2009). Fractional advection-dispersion equations for modeling transport at the Earth surface. *Journal of Geophysical Research*, *114*, F00A07. https://doi.org/10.1029/2008JF001246

Schwendel, A. C., Death, R. G., Fuller, I. C., & Joy, M. K. (2011). Linking disturbance and stream invertebrate communities: How best to measure bed stability. *Journal of the North American Benthological Society*, *30*(1), 11–24. https://doi.org/10.1899/09-172.1

Singh, A., Fienberg, K., Jerolmack, D. J., Marr, J., & Foufoula-Georgiou, E. (2009). Experimental evidence for statistical scaling and intermittency in sediment transport rates. *Journal of Geophysical Research*, *114*, F01025. https://doi.org/10.1029/2007JF000963

Tsujimoto, T. (1978). Probabilistic model of the process of bed load transport and its application to mobile-bed problems, Ph.D. thesis, Kyoto University, Kyoto, Japan.

Voepel, H., Schumer, R., & Hassan, M. A. (2013). Sediment residence time distributions: Theory and application from bed elevation measurements. *Journal of Geophysical Research: Earth Surface*, *118*, 2557–2567. https://doi.org/10.1002/jgrf.20151

Voller, V. R., & Paola, C. (2010). Can anomalous diffusion describe depositional fluvial profiles? *Journal of Geophysical Research*, *115*, F00A13. https://doi.org/10.1029/2009JF001278

Weeks, E. R., Urbach, J. S., & Swinney, H. L. (1996). Anomalous diffusion in asymmetric random walks with a quasi-geostrophic flow example. *Physica D: Nonlinear Phenomena*, *97*(1–3), 291–310. https://doi.org/10.1016/0167-2789(96)00082-6

Wong, M., Parker, G., DeVries, P., Brown, T. M., & Burges, S. J. (2007). Experiments on dispersion of tracer stones under lower-regime plane-bed equilibrium bed load transport. *Water Resources Research*, *43*, W034403. https://doi.org/10.1029/2006WR005172

Zeng, L., & Chen, G. Q. (2011). Ecological degradation and hydraulic dispersion of contaminant in wetland. *Ecological Modelling*, *222*(2), 293–300. https://doi.org/10.1016/j.ecolmodel.2009.10.024